

# Progress in the Development of a High-performance, Head Gradient Coil

John P. Staab<sup>1</sup>, Michael Stringer<sup>1</sup>, Sid Shevgoor<sup>1</sup>, Glenn N. Doty<sup>1</sup>, L. Wald<sup>2</sup>, J. L. Ackerman<sup>2</sup>, and F. David Doty<sup>1</sup>

<sup>1</sup>Doty Scientific, Columbia, SC, USA, <sup>2</sup> Massachusetts General Hospital, Charlestown, MA

## Synopsis

Available gradient coils have inadequate continuous gradient capability for some applications at high fields, such as diffusion weighted imaging, non-<sup>1</sup>H imaging, and microscopy using small rf coils for specific regions in the head and neck. There is also strong motivation for reducing acoustic noise from high-field gradient coils [1-3]. Here, we report our progress in the development of a novel head gradient coil incorporating 3D windings, ceramic formers, and direct water flooding of current elements, with thin polymeric coatings for electrical isolation, to address these issues.

A dimensionless approach to multi-parameter gradient optimization, that fully incorporates resistance, inductance, shielding, gradient uniformity, gradient magnitude, and null point, and approximately incorporated acoustic output, nerve stimulation, and some manufacturing issues, was found to have deficiencies treating thermal, acoustic, and manufacturing issues in the global optimization of a high-performance head gradient coil. These issues are being addressed by coupling of computational fluid dynamics (CFD), FEA, and manufacturing process optimization to the magnetic optimization problem.

Acoustic noise in the prototype for a standard EPI sequence was 110 dB, scaled to 3 T. The goal of developing a higher-performance, quieter head gradient coil is beginning to appear within reach.

## Head Gradient Coil Design Objectives

- Maximize continuous gradient capability (70 mT/m)
- Minimize acoustic noise
- Minimize nerve stimulation
- Improve reliability in very high fields (3-9.4 T)
- Minimize settling time
- Accommodate larger rf coils (36 cm grad coil ID)
- 24 cm dsv ROU (Region of Uniformity)
- ROU extending to within 9 cm of shoulder edge
- Incorporate high-order shims (Z2, Z3, Z4)
- Limit system cost (drivers plus coil)
- Keep axially symmetric, for general magnet compatibility

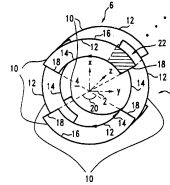
## Limitations of “Finger-Print” Coils

Roemer and many other researchers have shown that “finger print” coil patterns allow optimization of switching efficiency, gradient uniformity, and shielding effectiveness when length is not severely constrained. However, the current concentrations in the high-density regions limit power handling, and local forces and vibration are extremely high in the hot spots, often leading to early failure.

## 3D Winding Geometries and Acoustic Noise

Another major problem with conventional gradient coils, constrained to cylindrical surfaces, is that they can be very noisy, as large local forces and torques are generated, even though net torques and forces on the coil system are normally very nearly zero.

There have been many previous attempts to reduce acoustic noise. The approaches have included rigidization, acoustic barriers, vacuum insulation, supports at vibrational nodes, soft pulses, and so-called force cancellation, in which there is a deliberate attempt to add wire-coupled current elements having oppositely directed forces in ways to reduce local wire motion.



Since the net torque and net force acting on a current loop of arbitrary shape in a plane having its normal aligned with a uniform external  $B_0$  vanishes, several researchers have proposed the use of planar arc loops as a means of reducing acoustic noise. Unfortunately, this approach, as proposed by Mansfield, has serious deficiencies in efficiencies, shielding, and manufacturability. Similar challenges have beset most alternative designs with 3D windings.

## A Practical Design Approach

We showed seven years ago that combinations of wire-wound Golyay (saddle-type) coils and our crescent coils permitted higher switching and DC efficiencies than optimized patterns confined to cylindrical surfaces for the case of short gradient coils. Hence, we confined our optimization search to the use of such.

The addition of the shoulder-edge proximity constraint to the rest of the gradient design criteria (see “Design Objectives” above) makes the head-coil global optimization problem extremely complex. Cooling and manufacturability must be an integral part of the design.



## Full Parameter Set, Dimensionless Analysis

Closed-form analytical approaches to gradient optimization have not been shown to be capable of incorporating either heating or acoustic issues, nor have they been shown to be capable of handling a combination of surface current distributions and 3D winding geometries. Hence, our approach was to develop robust, flexible, powerful software (dubbed “COILS”) with simplex optimization capabilities. The  $B$  and  $A$  fields, resistance  $R_G$ , inductance  $L$ , forces, torques, induced potentials, and gradients  $G$  can easily be calculated by numerical methods from elementary laws (vector potential, Biot-Savart equation, Ohm’s law, and various basic relationships) for any set of conductors with known currents.

We have found the use of dimensionless parameters to be the most effective approach to gradient coil system optimization [4]. The five most important parameters are:

- (1) switching efficiency  $\eta_S$  – the ratio of magnetic energy within the ROU to the total magnetic energy,
- (2) rms gradient deviation within the ROU,
- (3) shielding effectiveness (ratio of internal to external energy),
- (4) DC efficiency (in combination with cooling effectiveness, this determines continuous gradient capability), and
- (5) acoustic efficiency,

Switching Efficiency,

$$\eta_S = \frac{\alpha^2 d_s^3 h_s^2}{\mu_0 L}$$

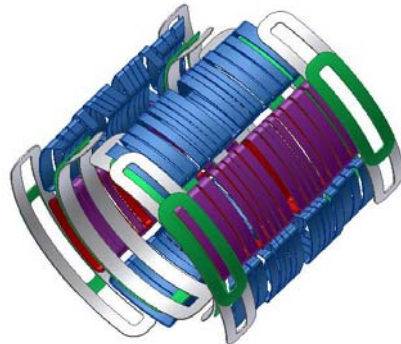
Where  $\alpha$  is the gradient gain (mT/m/A),  $d_s$  is the diameter of the ROU, and  $h_s$  is the axial length of the ROU.

- Gradient non-uniformity:  $\sigma_x(r) = (\nabla B_z(r) \cdot \nabla x - G_x) / G_x$

Eddy currents:  $\eta_{EC} = G_E / G_P \cdot 100\%$

DC efficiency:

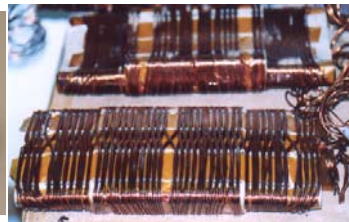
$$\eta_L = \frac{200\alpha^2 d_s^3 h_s}{\mu_0 R_E}$$



## The Doty Crescent-coil Design

Eight, crescent-shaped coils (six are shown above) are wound on crescent-forms (not shown) and attached around the perimeter of a ceramic former. Two of these crescent-forms are aligned on the Y-axis, for example. Another four crescent-forms are 45° off-axis and contain (blue) windings for both axes with proper phasing of the X and Y coils.

A key advantage of this approach compared to others using 3D windings is that switching efficiency may be improved by up to a factor of three by (a) using inclined arc loops that reduce the surface current density on the outside relative to that on the inside and (b) combining the crescent coils in an optimized way with heavy Golyay (saddle-type) coils at the ends. The severe over-shielding near the center that characterizes other force-canceled designs is eliminated, and shielding is actually better (usually by a factor of three) than normally obtained from short “finger-print” designs



The photo above shows the complete primary assembly mounted on the alumina ceramic (white cylinder) former without the external shield windings. Most of the windings comprise 2 parallel, 13 gage wires with quad-build polyimide coatings, and the two sides are further paralleled. The wires are bonded to the forms with Epo-Tek OM125 and then given several coatings of Epo-Tek 301-2 for moisture protection and high voltage insulation, as the windings are cooled by direct, forced flooding over all winding surfaces. The next version will utilize chemical vapor deposition of parylene for improved moisture resistance and high voltage insulation.

## An Approach to Acoustic Noise Predictions

Both bars (as in crescent coil forms) and cylinders (as in the main formers) exhibit transverse vibrational modes, as illustrated below, left. The first bending mode  $\omega_b$  for the thin-walled cylinder with free ends is given by the following equation, where  $r_f$  is the form radius,  $c_t$  is the velocity of transverse acoustic waves, and  $h$  is the axial length.

$$\omega_b \approx \frac{5r_f c_t}{h^2}$$

Approximate expressions for electro-mechanical efficiency  $\eta_{EM}$  (which we define as the ratio of total mechanical energy to magnetic energy within the ROU) can be readily derived for simple cases well below and well above  $\omega_b$  [4]. It is always found to be higher above  $\omega_b$  than below, and it is higher yet near the mechanical resonances. Hence, the first general rule is to maximize the resonant frequencies, which is done primarily by choosing materials with high acoustic velocities. Using a alumina ceramic former allows a factor of five increase in  $\omega_b$  (to 5 kHz) when proper care is taken to limit mass at critical locations. The estimated value of about 6 kHz agreed fairly well with the experimentally measured value of a little over 5 kHz. Mechanical efficiency below  $\omega_b$  decreases linearly with coilform stiffness.

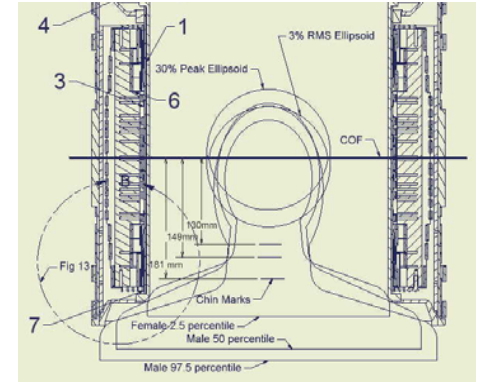
The inclined arc-loops in our crescent coils generate relatively small torques, as they are nearly perpendicular to  $B_0$ . Since the forms on which they are wound are extremely rigid (G10 fiberglass), we ignored their contribution to acoustic noise. Experimentally, the total acoustic noise from the crescent coils was found to be only about 6 dB below that from the Golyay coils mounted on the ceramic former over the 0-3 kHz range. Preliminary simulations suggest their lowest resonant mode is ~2.2 kHz.

## Preliminary Acoustic Test Results

Preliminary testing of the coil was carried out in a 1.5 T magnet with the results scaled appropriately (increased by 6 dB) to simulate 3 T. Published data, either at 3 T or appropriately scaled to 3 T, are also listed in the table below. The new coil will be slightly quieter than the best reference case. Known bonding problems with the Golyay coils may have played a role in not achieving the expected noise reduction, though pulse currents at over 250 A (35 mT/m) in the 1.5 T magnet did not produce hard evidence of such. The next step will be to carry out detailed finite element analysis (FEA) of the electromechanical/acoustic problem to gain further insights. Most significantly, methods of improving damping have not yet been carefully explored.

Acoustic Noise for EPI, 3 T, 20 mT/m, 120 mT/m/ms, 24 cm FOV, 64x64

Coil	Ref.	ID	Waveform	$f_0$	SPL
		cm		Hz	dB
Siemens, Sonata	1	68	trapezoidal	780	114
Varian, head	2	35	trapezoidal	~800	117
Bowtell, head	3	35	sinusoidal	1900	128
Doty, this work		36	trapezoidal	780	110



Fiberglass strips hold the Golyay windings slightly off the ceramic former to permit cooling water flow under, over, and between layers. Computational Fluid Dynamics (CFD) was used to analyze the water flow problem and improve the flow distribution between the parallel paths. Measured peak winding surface temperature at 200 A continuous, 50 minute test, Y axis primary, was 16°C above the inlet water temperature at a flow rate of ~9 gal/min (0.5 kg/s). This was ~ 20% higher than expected, and suggests the continuous gradient, single axis, for this prototype should be limited to 60 mT/m for 15 gal/min water flow rate.

## Head Coil Performance Comparisons

	Units	Roemer	Mansfield	Siemens	Doty
Grad. Gain, $\alpha$	mT/Am	0.138	0.084	0.08	0.138
L	$\mu$ H	240	354	160	255
$R_E$	W	0.22	0.25	0.1	0.17
Slew, $V_{\alpha} / L @ 670V$	-	380	156	335	365
Peak grad @ 800A	mT/m	110	67	64	110
Continuous Grad, $G_C$	mT/m	20	10	35	70
Shielding, eddies	%	2.5	38		0.1
Grad. Null point, $z_0$	mm	147	182		158
Front edge to ROU	mm	96	54		90
Dia. for $\sigma_{ms} = 9\%$	mm	240	240	~230	240
Lgh. for $\sigma_{ms} = 9\%$	mm	236	260	~220	240
S. Eff. $\eta_S$ for $\sigma_{ms} = 9\%$	%	4.97	1.38	~2	5.57

## CONCLUSIONS

Through bench tests and preliminary testing at 1.5 T confirmed the validity of the electromechanical and thermal design. In head coils, the use of 3D windings with efficient cooling permits substantially increased gradient strength, the use of smaller amplifiers, reduced eddy currents, and larger FOV. However, only a 7 dB reduction in acoustic noise, relative to the best prior published head-coil data to our knowledge, has thus far been achieved. Future work will utilize detailed FEA to gain an improved understanding of the primary mechanisms of noise generation in this coil. At the same time, more extensive testing of this prototype will be carried out at 3 T and higher fields to assess reliability as well as all performance specifications. A simplified analysis suggests future technical improvements may permit significant further reductions in noise reduction.

## REFERENCES

1. K Mechefske, R Geris, JS Gati, and BK Rutt, “Acoustic noise reduction in a 4T MRI scanner,” *Magn. Res. Mat. in Physics*, 13, 172-176, 2002.
2. L Price, JP DeWilde, AM Papadakis, JS Curran, and RI Kitney, “Investigation of Acoustic Noise on 15 MRI Scanners... to 3 T,” *JMRI*, 13:288-293, 2001.
3. R Foster, DA Hall, AQ Summerfield, AR Palmer, and RW Bowtell, “Sound-Level Measurements and Calculations of Safe Noise Dosage During EPI at 3T,” *JMRI*, 12:157-163, 2000.
4. D Doty, “Optimization of MRI Gradient Coils” in Spatially Resolved Magn. Reson., Ed. by P. Blumier et al, Wiley-VCH, Weinheim, 1998.
5. Wu, BA Chronik, C Bowen, C Mechefske, and BK Rutt, “Gradient-Induced Acoustic and Microscopic Field Fluctuations in a Whole Body Imager,” *MRI*